JOURNAL OF Applied Polymer SCIENCE

Electrochemical Supercapacitor Properties of Polyaniline Thin Films in Organic Salt Added Electrolytes

Yongcheol Jo,[1] Won-Je Cho,[2] A. I. Inamdar,[1] Byung Chul Kim,[3] Jongmin Kim,[1] Hyungsang Kim,[1] Hyunsik Im,[1] Kook-Hyun Yu,[2] Dae-Young Kim[3]

[1]Division of Physics and Semiconductor Science, Dongguk University, Seoul 100-715, Korea
[2]Department of Chemistry, Dongguk University, Seoul 100-715, Korea
[3]Department of Biological and Environmental Science, Dongguk University, Seoul 100-715, Korea
Correspondence to: H. Im (E-mail: hyunsik7@dongguk.edu) or K.-H. Yu (E-mail: yukook@dongguk.edu)

ABSTRACT: We demonstrate optimized supercapacitive characteristics of electrodeposited polyaniline by adding organic salt into electrolyte. The optimum amount of the organic salt is found to be 2 wt % which provides better ionic conductivity of the electrolyte, leading to the improved specific capacitance of 259 Fg^{-1}. This capacitance remains at up to 208 Fg^{-1} (80% capacity retention) after 1000 charge–discharge cycles. The optimized organic salt added electrolyte causes better rate performance and higher cyclability. Significantly reduced electrochemical charge transfer resistance at the electrode/electrolyte interface results in the increased ionic conductivity, which can be useful in electrochemically preferred power devices for better applicability. © 2013 Wiley Periodicals, Inc. J. Appl. Polym. Sci. **2014**, *131*, 40306.

KEYWORDS: conducting polymers; ionic liquids; electrochemistry

Received 26 September 2013; accepted 15 December 2013
DOI: 10.1002/app.40306

INTRODUCTION

Conducting polymers have attracted particular interest for supercapacitor due to good electrical conductivity and large pseudocapacitance.[1–3] The polymers represent an important class of electrode for the study of supercapacitors. The redox process which reversibly stores and releases charges is the main phenomenon in conducting polymer pseudocapacitors. The fast charge/discharge processes associated with conducting polymers enabled high specific power.[3] Conducting polymers have been known to deliver higher specific capacitance than carbon materials, since they store charges through both double-layer and redox capacitive mechanisms.[4] For the use of electrodes different kinds of composite polyaniline (PANI) films have been synthesized such as carboxyl-functionalized graphene oxide–PANI,[5] activated carbon cloth/PANI flexible electrode,[6] PANI/multi-wall carbon nanotube nanocomposites,[7,8] hybrid multilayer thin film supercapacitor of graphene nanosheets with PANI,[9] polypyrrole/carbon aerogel composite,[10] flexible graphene–PANI composite paper,[11] H^+, Fe^{3+} co-doped PANI/MWCNTs nanocomposite,[12] PANI/$MnWO_4$ nanocomposites.[13] On the other hand, carbon and graphene based electrodes have been extensively studied for the supercapacitive properties such as paper-based carbon nanotube,[14] reduced graphene oxide/ZnO nanorods/reduced graphene oxide on flexible polyethylene therephthalate (PET),[15] and In_2O_3 nanowire/carbon nanotube heterogeneous films.[16] From the literature it is generally accepted that the capacitance of an electrode is mainly determined by the following factors: (i) the morphology of the electrode, which provides good redox capacity, (ii) high conductivity (low charge transfer resistance), and (iii) porosity which provides high surface area. Electropolymerization is very advantageous because (i) in this process polymerization and doping processes exist simultaneously, (ii) polymerization rate can be controlled easily by adjusting applied potential, (iii) the applied constant potential in CA is useful for the uniform and adherent film deposition. Several research groups have studied the potentiostatic electro polymerization on ITO glass substrates using a three electrode electrochemical cell.[17,18] They choose the oxidation potentials for the PANI film deposition in the range of 0.6–0.75 V. The optical activity, crystallinity, and morphology of the PANI film can be controlled by varying oxidation potential during electro-polymerization.[19]

Ionic liquids/organic salt have attracted much attention due to their many unique physiochemical properties such as negligible vapor pressure, good dissolving ability, high ionic conductivity,

Additional Supporting Information may be found in the online version of this article.

and wide electrochemical window.[20,21] They have been used in various fields such as electrochemistry[22,23] and biochemistry[24] as solvents, reaction mediums, catalysts, and functional materials. However, to our best knowledge, the use of organic salt as an additive to reduce the electrochemical charge transfer resistance in PANI-based supercapacitor applications has not been reported yet. In this work, we have used self-prepared dicationic organic salt in an acidic electrolyte for the electrochemical supercapacitor measurements of electro-polymerized PANI thin films. We demonstrate the effect of the organic salt (at different wt %) in the electrolyte on the electrochemical and supercapacitive properties of the PANI thin films.

EXPERIMENTAL

PANI thin films were synthesized using the electrodeposition (ED) technique by polymerization of aniline and sulfuric acid. The films were deposited on conducting glass substrate coated with indium-doped tin oxide (ITO, 25–27 Ω/cm^2). Prior to the deposition, the ITO substrates were ultrasonically cleaned consecutively in acetone, methanol, and deionized water. The reaction bath for the PANI film deposition contains 0.2*M* aniline (Extra Pure, Yakuri Pure Chemical Co. Ltd.) and a 0.2*M* H_2SO_4 (Extra pure, DAEJUNG Chemicals and Metals Co. Ltd.) solution. PANI films were electrodeposited using a three-electrode electrochemical system in which ITO glass substrate was used as the working electrode, graphite as the counter electrode, and a saturated calomel electrode (SCE) as the reference electrode. ED was carried out at 0.75 V (versus SCE) for 20 min, using a chronoamperometry (CA) technique at room temperature.[25] Similarly, the PANI films were grown on ITO substrates by potentiostatic electro-polymerization process at 0.7 V.[26] To remove loosely adhered PANI, the films were immersed in deionized water and dried in natural air. The synthesis of N^1,N^1,N^1,N^6,N^6,N^6-hexamethylhexane-1,6-diaminiumtetrafluoroborate ($C_6((TMA)(BF_4))_2$) organic salt (OS) was carried out by using trimethylamine mixed with 1,6-dibromohexane in ethanol (see Supporting Information for details). The electrochemical capacitance performance of the PANI film was evaluated using cyclic voltammetry (CV), galvanostatic charge/discharge method, and AC impendence analysis. A potentiostat (Princeton Applied Research, VersaSTAT 3) was used as a three-electrode electrochemical cell containing 0.5*M* $LiClO_4$ + propylene carbonate (PC) as the electrolyte, a PANI electrode as the working electrode, SCE as the reference electrode, and graphite as the counter-electrode.

A pure 0.5*M* $LiClO_4$ electrolyte was prepared in a non-aqueous propylene carbonate electrolyte by adding 5.31 g of lithium perchlorate anhydrous (Samchun pure chemicals Pvt. Ltd.) in 100 mL of propylene carbonate electrolyte at room temperature. The electrochemical experiments were performed in four different electrolytes containing different wt % of the organic salt: 0, 1, 2, 3 wt % in 0.5*M* $LiClO_4$ + PC electrolyte. These electrolytes will be denoted hereafter as 0 wt % OS, 1 wt % OS, 2 wt % OS, and 3 wt % OS with increasing wt % of the organic salt. It seems to be very difficult to dissolve more than 3 wt % of the organic salt in the non-aqueous propylene carbonate electrolyte due to the solubility limit of the electrolyte. The ionic conductivity of the pure electrolyte is 6.54 mS cm^{-1}, but it is 6.99, 7.58, and 7.26 mS cm^{-1} after the addition of 1, 2, and 3 wt % of the organic salt, respectively. The decreased ionic conductivity of the 3 wt % electrolyte is presumably due to the decreased movement of ions which is caused by the increased viscosity of the electrolyte. The charge–discharge measurement was performed according to the order of electrode-electrolyte-electrode i.e. a symmetric capacitor made of two PANI films as electrodes (Figure 1). A potentiostat/glavanostate (model WMPG 1000) was used in the galvanostatic mode to record the charging and discharging characteristics of the supercapacitor thin films. The films' morphological properties were characterized using field emission scanning electron microscopy (FE-SEM, Model: JSM-6701F, JEOL, Japan).

RESULTS AND DISCUSSION

Figure 1 shows the SEM morphological image of the electrodeposited PANI electrode and schematic of the supercapacitor

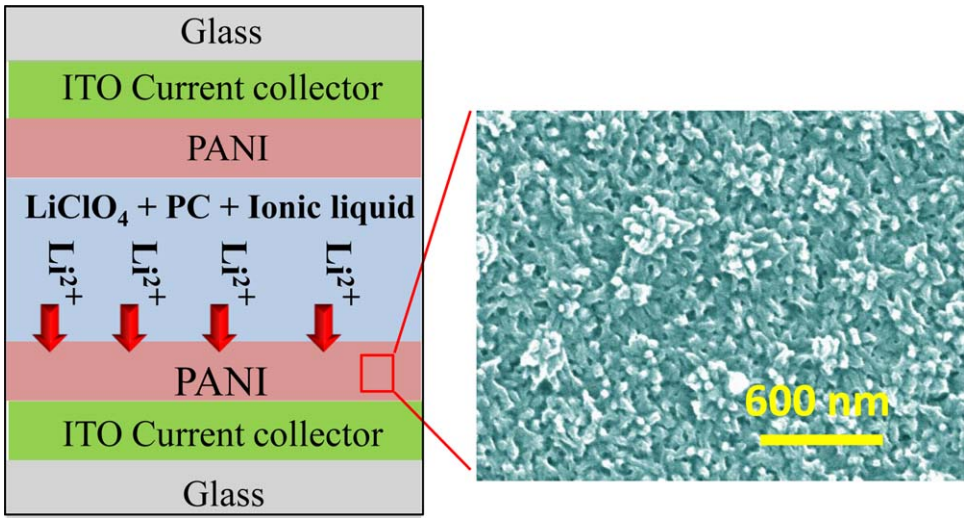

Figure 1. Schematic of a PANI-based electrochemical supercapacitor device (left) and scanning SEM image of electro-polymerized PANI thin film (right). [Color figure can be viewed in the online issue, which is available at wileyonlinelibrary.com.]

device structure. The SEM image depicts cauliflower-like porous morphology. The thickness of the electrode film is found to be 120 nm from the cross-sectional SEM image. The films electrodeposited at 0.75 V (versus SCE) using a chronoamperometry (CA) technique at room temperature show a pure PANI structure confirmed by FITR measurements.[27] Figure 2(a) shows the 1st cycle of the CV curves recorded at a scan rate of 100 mV s^{-1}. The potential window is fixed from0.0 V to 1.0 V (vs SCE).The shape of the measured CV curve provides crucial information on the oxidation–reduction reaction of the PANI electrode. Two pairs of redox peaks observed in the CV curves indicate the transition between leucoemeraldine and emeraldine, and for emeraldine salt and pernigraniline of PANI.[25] The capacitance is mainly due to the redox reaction and the shape of the CV curves is distinguished from that of electric double-layer capacitors, which is normally close to an ideal rectangle. The increased contribution of the redox reaction from the CV curves is observed after addition of organic salt into the electrolyte. The current/voltage slope in the CVs indicates the magnitude of the materials conductivity.[28] The highest slope for the CVs is observed for the one with the 2 wt % OS, indicating a better electrical conductivity of the electrolyte. The PANI electrodes exhibit two pairs of redox peaks (wavy shape in the CVs) in all four different electrolytes, which are indicative of a pseudocapacitive characteristic of PANI. The peak at around 0.15 V (vs SCE) is attributed to the transition of PANI from the semiconducting state to the conducting state, whilst the peak at around 0.85 V (vs SCE) is due to transition from the emeraldine to the pernigraniline.[29] The current density of the CVs is increased with increasing wt % of the OS up to 2 wt %. This indicates that the charge storing capacity is high in the 2 wt % OS electrolytes. The increase in the current density up to 2 wt % addition of OS may be due to the increased ionic conductivity and 2 wt % OS seems to be optimal with regard to the current density and supercapacitive properties. This increased ionic conductivity of the electrolyte may be due to the decrease in the solvent viscosity of the electrolyte after the addition of OS. Another possible reason for the increase in the ionic conductivity of electrolyte may be due to the polar interaction between the polyanionic PANI and the OS, which reduces the coulombic interaction of charge carriers. There could be the possibility of the formation of micelle in the electrolyte after addition of organic salt. Two wt % of the organic salt is the critical micelle concentration (CMC) which greatly increases the conductivity of the electrolyte. Beyond CMC value (2 wt % of the organic salt), the decrease in the conductivity can be attributed to the formation of crosslinks among micelles i.e., transient network.[30] The performance of the electrochemical supercapacitor is crucially dependent on its conductivity and wettability. The electrochemical supercapacitor stores energy using either ion adsorption or fast surface redox reactions at the surface. These redox reactions occur due to the reversible Faradaic charge-transfer at the electrode–electrolyte interface. The addition of organic salt increases the ionic conductivity which improves the electroactivity (redox reaction rate) of the electrolyte.

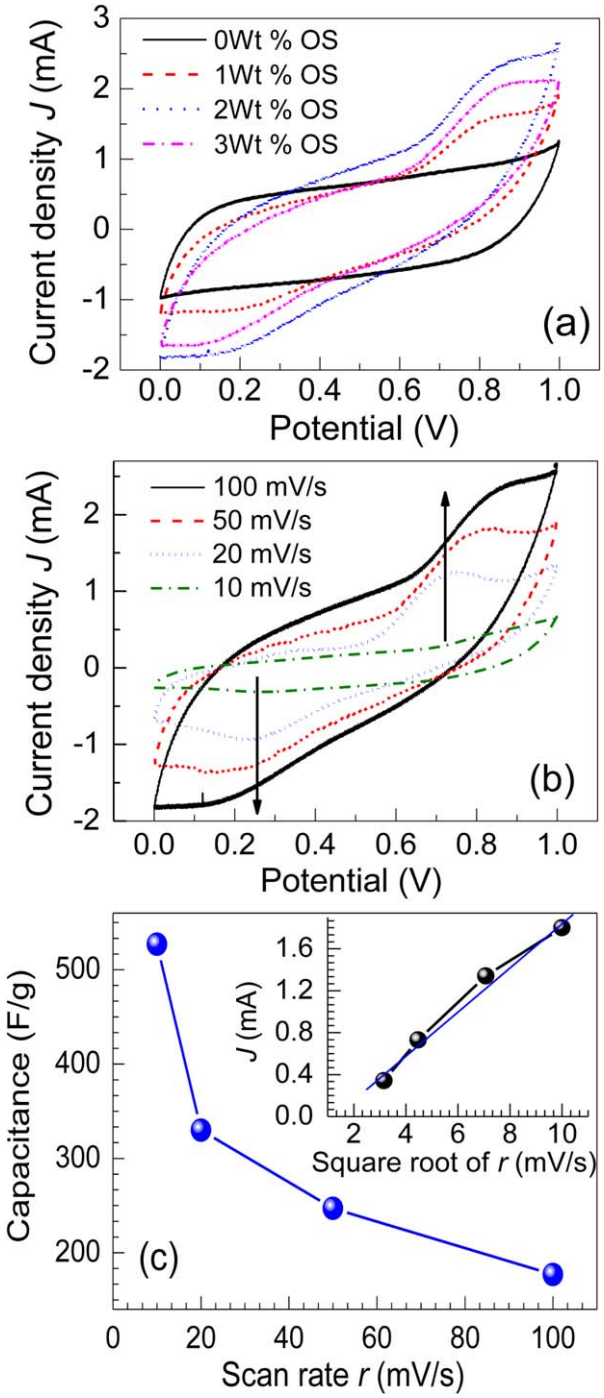

Figure 2. (a) Cyclic voltammograms of an electrodeposited PANI film recorded in four different electrolytes at a scan rate of 100 mV s^{-1}. (b) Cyclic voltammograms in the 2 wt % OS electrolyte at scan rates of 10, 20, 50, and 100 mV s^{-1}; (the arrows indicate the increasing scan rate). (c) Determination of specific capacitance at different scan rates. The inset shows the dependence of current density with square root of scan rate. [Color figure can be viewed in the online issue, which is available at wileyonlinelibrary.com.]

Figure 2(b) shows the CV curves of the PANI film in the 2 wt % OS electrolyte at four different scan rates of 10, 20, 50, and 100 mV s^{-1}. As the scan rate is increased, the current of the CVs also increases. The retention in the CV shape and redox peaks without apparent deviation at different scan rates

indicates good electrochemical reversibility of the PANI thin film. This result can be understood by considering the Randles–Sevcik equation.

$$I_P = K\ n^{3/2} A\ D^{1/2} M r^{1/2} \quad (1)$$

where the constant $K = 2.69 \times 10^5$ C/(mol×V$^{1/2}$), n is the number of electrons transferred in the redox process, A is the area of the electrode in cm^2, D is the diffusion coefficient in cm^2 s^{-1}; M is the solution concentration in mole cm^{-3}, and r is the scan rate of the potential in V s^{-1}. This equation describes the current of the electrochemical redox reaction as linearly proportional to the concentration of electroactive species and square root of the scan rate. The positive shift in the oxidation peak (indicated by dashed arrows) and the negative shift in the reduction peak (indicated by dashed arrows) with increasing scan rate are due to the increased resistance of the electrode.[31]

The redox capacitance of the PANI thin film is determined from the CV curves at different scan rates in the 2 wt % OS electrolyte by using the following equation,

$$C_{sp} = \frac{i}{r \times m} \quad (2)$$

where i is the average cathodic current, r is the scan rate, and m is the mass of the active electrode. Figure 2(c) shows the plot of the capacitance versus scan rate of the PANI thin film. The specific capacitance value is found to be 527 Fg^{-1} at a scan rate of 10 mV s^{-1} whereas it decreases to 177 Fg^{-1} at a scan rate of 100 mV s^{-1}. The obtained capacitance values are higher than that of previously reported specific capacitance of the PANI measured in $LiClO_4$+PC electrolyte.[2] These values are even higher than those measured in acidic electrolytes like 1*M* H_2SO_4.[32–34] The inset shows the graph of the reduction peak current density versus the square root of the scan rate for the PANI thin film measured in the 2 wt % OS electrolyte. The reduction peak current density versus scan rate plot matches well with a fitted straight line. The linear relationship between the current and the square root of the scan rate demonstrates the diffusion-controlled reaction for the PANI thin film.[25]

The charge–discharge (CD) characteristics of the PANI film are investigated using chronopotentiometry from 0 to 1 V at an applied current density of 0.5 mA cm^{-2}. A supercapacitor was constructed using two PANI thin films as electrodes. The two PANI electrodes were held 2 cm apart from each other and a 1 cm length was dipped into the electrolyte. The corresponding results are shown in Figure 3 (a). All the charging curves recorded in different electrolytes are linear in nature. The discharge curve contains two slopes: one is parallel to the *y*-axis, which represents the voltage change, and the second slope is related to the capacitive component [Figure 3(a)]. The deviation from the symmetrical triangular shape of the charge–discharge curve indicates the existence of the Faradaic reaction at the

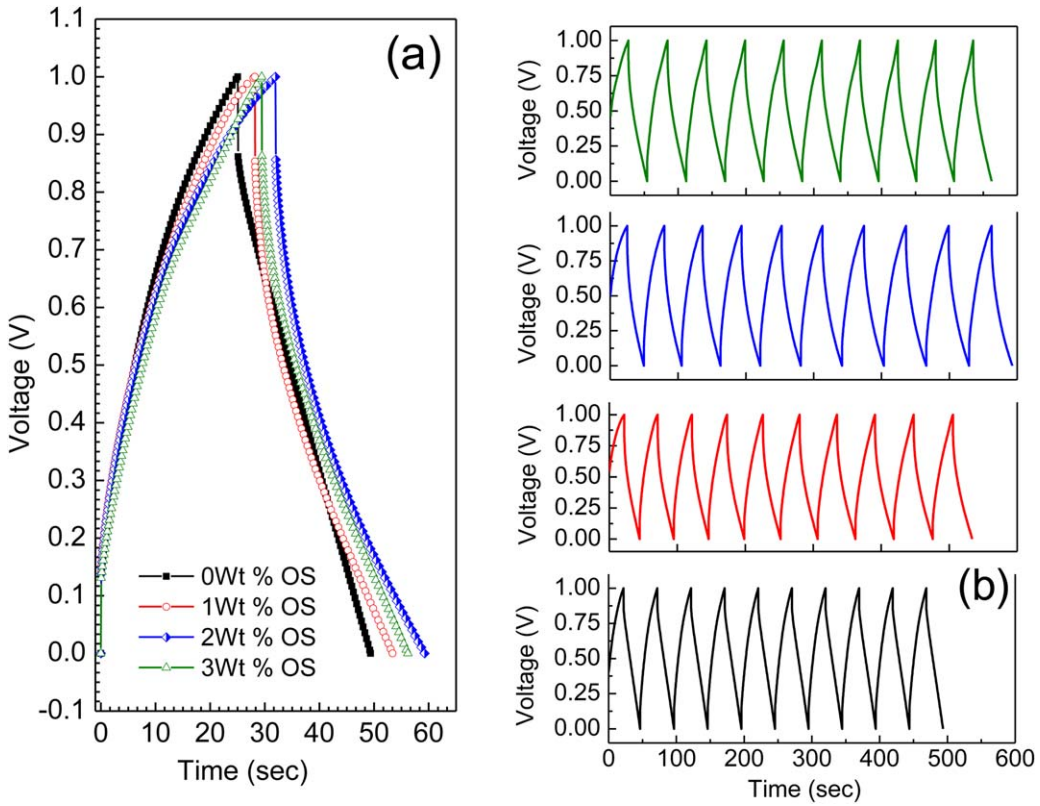

Figure 3. Galvanostatic charge/discharge measurements of the PANI electrode within the potential window of 0 to 1.0 V (vs. SCE) at a current density of 0.5 mAg^{-1}. (a) Voltage-time profile of PANI electrode measured in four different electrolytes. (b)Long-term charge/discharge measurement of PANI electrode in four different electrolytes. [Color figure can be viewed in the online issue, which is available at wileyonlinelibrary.com.]

surface of the supercapacitive electrodes.[10] It can be seen that the charging and discharging times are higher in the CD curve measured in the 2 wt % OS electrolyte. The specific capacitance of the electrode can be evaluated according to the following equation,[35]

$$Cs = \frac{I \times t}{\Delta V \times m} \quad (3)$$

where I is the charge–discharge current, Δt is the discharge time, ΔV is the electrochemical potential window, and m is the mass of the active material. The specific capacitance values are found to be 216 Fg^{-1} for the pure acidic electrolyte (0 wt % OS), 233 Fg^{-1} for the 1 wt % OS, 259 Fg^{-1} for the 2 wt % OS, and 246 Fg^{-1} for the 3 wt % OS. The highest capacitance value obtained using the 2 wt % OS electrolyte may be due to the most optimal ionic conductivity of the electrolyte which helps faster insertion and extraction of Li^{2+} ions into the electrode surface which greatly reduces the diffusion length.

The long-term charge–discharge measurements were also performed for the PANI thin film. Figure 3(b) shows the charge–discharge curves of the PANI thin film for the first 10 cycles in the different electrolytes. The charge/discharge curves exhibit reversible characteristics without apparent deviation in each cycle; this suggests good electrochemical stability for the PANI electrode in all four electrolytes. The coulombic efficiency of PANI electrode is also tested using the ratio of the discharge time to the charging time.[36] The PANI electrodes exhibit high coulombic efficiency above 85% in all four different electrolytes which indicates good rate capability and reversibility.

Figure 4 shows the electrolyte-dependent specific capacitances and capacity retention of the PANI sample for 1000 cycles. The highest specific capacitance value is obtained using the 2 wt % OS electrolyte. The specific capacitance obtained using the pure electrolyte is lowest and rapidly decreases with increasing charge–discharge cycles [Figure 4(a)]. The best capacity retention (~80% after 1000 cycles) is also obtained using the 2 wt % OS electrolyte while the poorest retention (~62%) is obtained using the pure electrolyte [Figure 4(b)]. These results demonstrate that the PANI film-based supercapacitor properties can be considerably improved by adding an optimal amount of organic salt in a conventionally used electrolyte.

Electrochemical impedance spectroscopy (EIS) measurements were carried out at 0.7 V. Figure 5 presents the Nyquist plot of the PANI film for the different electrolytes. The equivalent circuit diagram for the Nyquist plot is shown in the inset, where R_s, C_{dl}, R_{ct}, and w represent the series resistance, electrical double layer capacitance, charge transfer resistance, and Warburg impedance, respectively. The low-to-high direction of the frequency is indicated by the arrow. The Nyquist plot shows inclined lines approximately at around 45° in the low frequency region, which is characteristic of supercapacitive behavior, and the inclined curves at the high frequency region, indicate typical electric double layer behavior. The intersection to the x-axis in the high frequency region provides the quantitative values of the charge transfer resistance of the electrolyte. The charge transfer resistances of the electrolytes are found to be 88 Ω for the 0 wt %OS, 84 Ω for the 1 wt % OS, 76 Ω for the 2 wt %

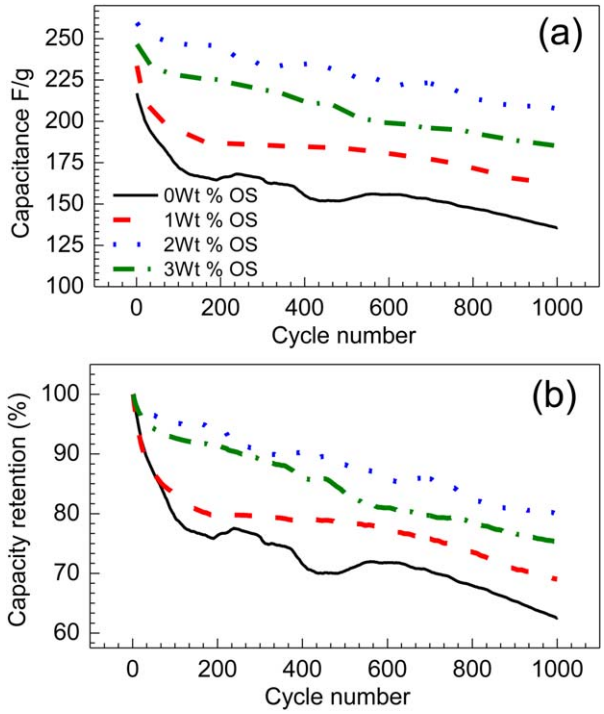

Figure 4. The specific capacitance of a symmetric capacitor made of two PANI films as electrodes, measured in charging–discharging cycles at a constant current of 0.5 mA. (a)Variation of specific capacitance of PANI electrodes as a function of cycle number for 1000 charge–discharge cycles. (b) Capacity retention properties for 1000 charge–discharge cycles. [Color figure can be viewed in the online issue, which is available at wileyonlinelibrary.com.]

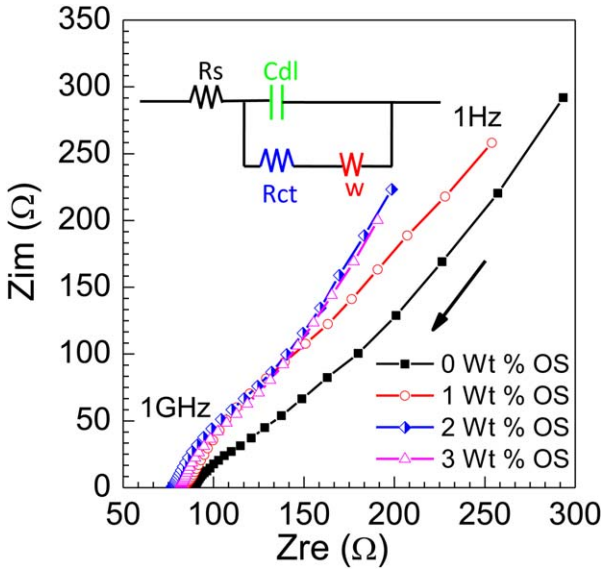

Figure 5. Impedance spectra of PANI electrodes in four different electrolytes. Nyquist plot of PANI electrodes at 0.7 V (vs SCE) open circuit potential in the frequency range of 1 GHz to 1 Hz. The inset shows the equivalent circuit diagram for the Nyquist plot. [Color figure can be viewed in the online issue, which is available at wileyonlinelibrary.com.]

OS, and 81 Ω for the 3 wt % OS. The decrease in the charge transfer resistance for the 2 wt % OS electrolyte is due to the increased ionic conductivity which causes reduction in the electrode/electrolyte interface resistance. These charge transfer reactions has certain speed, which depends on concentration of the reaction products and the potential, temperature, and kind of reaction. The higher equivalent series resistance (ESR) can affect the rate performance of the supercapacitor,[37] which is lowest for the 2 wt % OS electrolyte which shows better rate performance and higher cyclability. This decreased electrochemical resistance at the electrode/electrolyte interface is useful in electrochemically preferred power devices for better applicability.[6]

CONCLUSIONS

The supercapacitive properties of a PANI film are investigated using organic salt added acidic electrolyte. The optimum wt % of the organic salt which yields the best supercapacitor properties is found to be 2 wt %. The considerably improved specific capacitance of ~259 Fg^{-1} and ~80% capacity retention (~208 Fg^{-1}) after 1000 charge–discharge cycles are obtained. The increased ionic conductivity of the organic salt added electrolyte causes reduction in the electrode/electrolyte interface resistance which is useful in electrochemically preferred power devices for better applicability.

ACKNOWLEDGMENTS

This project was supported by the National Research Foundation (NRF) of Korea (Grant Nos. 2012-00109 and 2012-008517). DY Kim acknowledges a support from the Korea Ministry of Environment (Grant No. 412-112-011).

REFERENCES

1. Snook, G. A.; Kao, P.; Best, A. S.; *J. Power Sources* **2011**, *196*, 1.
2. Chaudhari, S.; Sharma, Y.; Sathyaseelan P.; Archana Jose, R.; Ramakrishna, S.; Mhaisalkar, S.; Srinivasan, M. *J. Appl. Polym. Sci.* **2013**, *129*, 1660.
3. Murugan, A. V.; Viswanath, A. K.; Campet, G.; Gopinath, C. S.; Vijayamohanan, K. *Appl. Phys. Lett.* **2005**, *87*, 243511.
4. Sivakkumar, S. R.; Kim, W. J.; Choi, J. A.; MacFarlane, D. R.; Forsyth, M.; Kim, D. W. *J. Power Sources* **2007**, *171*, 1062.
5. Liu, Y.; Deng, R.; Wang, Z.; Liu, H. *J. Mater. Chem.* **2012**, *22*, 13619.
6. Zhong, M.; Song, Y.; Li, Y.; Maa, C.; Zhai, X.; Shi, J.; Guo, Q.; Liu, L. *J. Power Sources* **2012**, *217*, 6.
7. Yoon, S. B.; Yoon, E. H.; Kim, K. B. *J. Power Sources* **2011**, *196*, 10791.
8. Liu, Q.; Nayfeh, M. H.; Yau, S. T. *J. Power Sources* **2010**, *195*, 7480.
9. Lee, T.; Yun, T.; Park, B.; Sharma, B.; Song, H. K.; Kim, B. S. *J. Mater. Chem.* **2012**, *22*, 21092.
10. An, H.; Wang, Y.; Wang, X.; Zheng, L.; Wang, X.; Yia, L.; Bai, L.; Zhang, X. *J. Power Sources* **2010**, *195*, 6964.
11. Cong, H. P.; Ren, X. C.; Wang, P.; Yu, S. H. *Energy Environ. Sci.* **2013**, *6*, 1185.
12. Ghosh, D.; Giri, S.; Mandal, A.; Das, C. K. *Appl. Surf. Sci.* **2013**, *276*, 120.
13. Saranya, S.; Selvan, R. K.; Priyadharsini, N. *Appl. Surf. Sci.* **2012**, *258*, 4881.
14. Shan, H.; Rajamani, R.; Yu, X. *Appl. Phys. Lett.* **2012**, *100*, 104103.
15. Guo, G.; Huang, L.; Chang, Q.; Ji, L.; Liu, Y.; Xie, Y.; Shi, W.; Jia, N. *Appl. Phys. Lett.* **2011**, *99*, 083111.
16. Chen, P. C.; Shen, G.; Sukcharoenchoke, S.; Zhou, C. *Appl. Phys. Lett.* **2009**, *94*, 043113.
17. Kim, Y. S.; Sohn, J. S.; Ju, H. R.; Inamdar, A. I.; Im, H.; Kim, H. *J. Korean Phys. Soc.* **2012**, *60*, 1767.
18. Guo, Y.; Zhou, Y. *Eur. J. Polym Sci.* **2007**, *43*, 2292.
19. Li. W.; Wang, H. L. *Adv. Funct. Mater.* **2005**, *15*, 1793.
20. Chiappe, C.; Pieraccini, D. *J. Phys. Org. Chem.* **2005**, *18*, 275.
21. Endres, F.; Abedin, S. Z. E. *Phys. Chem. Chem. Phys.* **2006**, *8*, 2101.
22. De Souza, R. F.; Padilha, J. C.; Goncalves, R. S., Dupont, J. *Electrochem. Commun.* **2003**, *5*, 728.
23. Wang, P.; Zakeeruddin, S. M.; Comte, P.; Exnar, I.; Gratzel, M. *J. Am. Chem. Soc.* **2003**, *125*, 1166.
24. Rantwijk, F. V.; Sheldon, R. A. *Chem. Rev.* **2007**, *107*, 2757.
25. Inamdar, A. I.; Kim, Y. S.; Sohn. J. S.; Im, H.; Kim, H.; Kim, D. Y.; Kalubarme, R. S.; Park, C. J. *J. Korean Phys. Soc.* **2011**, *59*, 145.
26. Wang, H. Z.; Zhang, P.; Zhang, W. G.; Yao, S. W. *Chem. Res. Chin. Univ.* **2012**, *28*, 133.
27. Yusairie, M.; Ruhani, I.; Muhammad, F. Z. *IEEE Symp.* **2012**, 1301.
28. Xu, F.; Zheng, G.; Wu, D.; Liang, Y.; Lia, Z.; Fu, R. *Phys. Chem. Chem. Phys.* **2010**, *12*, 3270.
29. Li, J.; Xie, H.; Li, Y.; Liu, J.; Li, Z. *J. Power Sources* **2011**, *196*, 10775.
30. Wang, S. C.; Wei, T. C.; Chen, W. B.; Tsao, H. K. *J. Chem. Phys.* **2004**, *120*, 4980.
31. Wang, Y. G.; Li, H. Q.; Xia, Y. Y. *Adv. Mater.* **2006**, *18*, 2619.
32. Palaniappan, S.; Sydulu, S. B.; Prasanna, T. L.; Srinivas, P. *J. Appl. Polym. Sci.* **2011**, *120*, 780.
33. Kuang, H.; Cao, Q.; Wang, X.; Jing, B.; Wang, Q.; Zhou, L. *J. Appl. Polym. Sci.* **2013**, *130*, 3753.
34. Tan, Y. T.; Ran, F.; Wang, L. R.; Kong, L. B.; Kang L. *J. Appl. Polym. Sci.* **2013**, *127*, 1544.
35. Mao, L.; Zhang, K.; Chan, H. S. O.; Wu, J. *J. Mater. Chem.* **2012**, *22*, 80.
36. Fan, H.; Wang, H.; Zhao, N.; Zhang, X.; Xu, J. *J. Mater. Chem.* **2012**, *22*, 2774.
37. Lei, Z.; Christov, N.; Zhao, X. S. *Energy Environ. Sci.* **2011**, *4*, 1866.